MCB
Journals.ASM.org

Activation of a Novel Ubiquitin-Independent Proteasome Pathway when RNA Polymerase II Encounters a Protein Roadblock

Yi Ban,[a] Chia-Wen Ho,[a] Ren-Kuo Lin,[a] Yi Lisa Lyu,[a] Leroy F. Liu[a,b]

Department of Pharmacology, Robert Wood Johnson Medical School, Rutgers University, Piscataway, New Jersey, USA[a]; College of Medical Science and Technology, Taipei Medical University, Taipei, Taiwan[b]

Topoisomerase IIβ (Top2β)-DNA cleavage complexes are known to arrest elongating RNA polymerase II (RNAPII), triggering a proteasomal degradation of the RNAPII large subunit (RNAPII LS) and Top2β itself as a prelude to DNA repair. Here, we demonstrate that the degradation of Top2β occurs through a novel ubiquitin-independent mechanism that requires only 19S AAA ATPases and 20S proteasome. Our results suggest that 19S AAA ATPases play a dual role in sensing the Top2β cleavage complex and coordinating its degradation by 20S proteasome when RNAPII is persistently stalled by the Top2β protein roadblock. Clarification of this transcription-associated proteasome pathway could shed light on a general role of 19S AAA ATPases in processing tight protein-DNA complexes during transcription elongation.

During transcription elongation, RNA polymerase II (RNAPII) frequently encounters various roadblocks (e.g., UV adducts, oxidized bases, and carcinogen-DNA adducts). Such an encounter has been demonstrated to elicit complex responses, including arrest of elongating RNAPII and degradation of its large subunit (RNAPII LS) (1–3). The arrest of RNAPII is evidenced by the accumulation of its hyperphosphorylated form, RNAPIIo (4), which is primarily due to the phosphorylation on both serine-2 (Ser-2) and serine-5 (Ser-5) of the RNAPII C-terminal domain (CTD) (5). The accumulation of RNAPIIo is followed by its ubiquitin (Ub)-dependent proteasomal degradation (6, 7).

Many cancer therapeutics (e.g., etoposide/VP-16 and doxorubicin) are known to stabilize topoisomerase-DNA cleavage complexes. It has been shown that the drug-stabilized topoisomerase IIβ (Top2β)-DNA cleavage complexes are localized on the transcribed region, triggering degradation of Top2β and subsequent exposure of DNA damages (8, 9). Mounting evidence indicates these Top2β-incurred DNA damages are the cause of severe side effects associated with VP-16 (etoposide)- or doxorubicin-based chemotherapy (10–12). Understanding this transcription-mediated Top2β degradation could contribute to a more efficacious use of VP-16 in the clinic. However, the molecular basis for the interplay among transcription elongation, proteasomal degradation, and the DNA damage signals awaits elucidation.

In recent years, many studies have linked proteasome to transcription (13–16). To date, the precise function of 19S AAA ATPases (ATPases associated with various cellular activities, hereafter referred to as 19S ATPases) and the 20S proteasome in transcription remains unknown. We employed Top2β-DNA cleavage complexes as a model system to study the encounter between elongating RNAPII and protein roadblocks. Our findings indicate that Top2β-DNA cleavage complexes arrest transcription elongation and induce a proteasomal degradation of Top2β on DNA. Surprisingly, such degradation takes a Ub-free route and requires only 19S ATPases and 20S proteasome.

MATERIALS AND METHODS

Chemicals, plasmid DNAs, siRNAs, and antibodies. VP-16 (etoposide) and 5,6-dichlorobenzimidazole riboside (DRB) were purchased from Sigma. MG132 was purchased from Boston Biochem. Staphylococcal S7 nuclease and Complete protease cocktail inhibitor tablets were purchased from Roche Molecular Biochemicals. Plasmids (pcDNA3.1) expressing hemagglutinin (HA)-tagged lysine-to-arginine mutant ubiquitins (i.e., K48R, K29R, and K63R) were obtained from Cam Patterson (University of North Carolina, Chapel Hill, NC). The plasmid that expresses a mutant ubiquitin in which all seven lysines were mutated to arginines (UbR7) was obtained from Michelle Pagano (New York University, New York). pcDNA3-based plasmids that express truncated shuttle factors (ΔUBL Rad23 and ΔUBA Rad23) were obtained from Christine Blattner (Karlsruhe Institute of Technology, Germany). Short interfering RNAs (siRNAs) targeting different proteasome subunits (Rpn2, Rpn11, Rpt5-Rpt6, S5a, and P28/Nas6) were purchased from Sigma-Aldrich. The control siRNA was purchased from Santa Cruz Biotechnology. Antibodies against RNAPII (Santa Cruz Biotechnology), Top2β (H8 [sc-25330], H-286 [sc-13059]) (Santa Cruz Biotechnology), proteasome subunits (Enzo Life Science), and γ-H2AX (Upstate Biotechnology) were all acquired from different commercial sources. Anti-hTop1 antibody was obtained from sera of scleroderma 70 patients as described before (17). The anti-Ub antibody was generated as described previously (18). The hybridoma cell line that produces monoclonal antibody 12G10 (against α-tubulin) was obtained from the Developmental Studies Hybridoma Bank. RNAPII monoclonal antibody H5 (specific to p-Ser-2) was obtained from Covance (MPY-127R).

Cell culture. Top2β$^{+/+}$ and top2β$^{-/-}$ primary mouse embryonic fibroblasts (pMEFs) were isolated from embryonic day 13.5 (E13.5) mouse embryos as described previously (11). Both pMEFs and HeLa Tet-On (Clontech) cells were cultured in a humidified atmosphere of 5% CO_2 at 37°C in Dulbecco's minimum essential medium (DMEM) containing 10% fetal bovine serum, L-glutamine (2 mM), penicillin (100 U/ml), and streptomycin (100 μg/ml). The temperature-sensitive mouse mammary carcinoma cell line ts85 (a ubiquitin E1 temperature-sensitive [ts] mu-

Received 4 April 2013 Returned for modification 14 May 2013
Accepted 17 July 2013
Published ahead of print 12 August 2013
Address correspondence to Yi Lisa Lyu, lyuyi@rwjms.rutgers.edu, or Leroy F. Liu, lliu@rwjms.rutgers.edu.
Supplemental material for this article may be found at http://dx.doi.org/10.1128/MCB.00403-13.

doi:10.1128/MCB.00403-13

tant) (19) was cultured in RPMI medium supplemented with the same formula as that described above at a permissive temperature of 30°C. For performing experiments at the nonpermissive temperature, ts85 cells were first cultured at 42°C for 20 min, followed by further incubation at a nonpermissive temperature of 39°C.

Construction of HA-tagged mTop2β expression vectors. Full-length mTop2β cDNA was generated using the total RNAs isolated from embryonic day 16 mouse brains by reverse transcription and PCR. The HA peptide was inserted between the first amino acid, methionine, and the second amino acid, alanine, of the mTop2β protein and cloned into the plasmid pCS2+ (pYLL201). The HA-tagged mTop2β containing the active-site tyrosine mutation (Y814F) was generated by PCR-based site-directed mutagenesis (pYLL204). To check the expression of HA-tagged mTop2β and HA-tagged mTop2βY814F, plasmids pYLL201 and pYLL204, respectively, were transfected into HeLa cells. The expression of full-length HA-tagged mTop2β was confirmed by immunoblotting using anti-Top2β or anti-HA antibody.

Immunoblotting. VP-16-induced Top2β degradation and camptothecin (CPT)-induced Top1 degradation were monitored by immunoblotting of the alkaline lysates prepared from drug-treated cells (8, 18), with slight modifications. Briefly, following inhibitor treatment, cells were washed 3 times with drug-free DMEM and incubated at 37°C in a CO_2 incubator for another 30 min (for the purpose of reversing topoisomerase cleavage complexes). Cells cultured in 35-mm dishes were then lysed with 100 μl of an alkaline lysis buffer (200 mM NaOH, 2 mM EDTA). Alkaline lysates were neutralized by the addition of 12 μl of 1 M HCl, 600 mM Tris, pH 8.0, followed by mixing with 13 μl of 10× S7 nuclease buffer (50 mM $MgCl_2$, 50 mM $CaCl_2$, 5 mM dithiothreitol, 1 mM EDTA, and a protease inhibitor cocktail) and 60 U of staphylococcal S7 nuclease. The resulting mixtures were incubated on ice for 35 min for releasing Top2β from Top2β-DNA covalent complexes. Forty microliters of 6× SDS gel sample buffer was added to each sample. The lysates were boiled for 10 min, analyzed by SDS-PAGE, and immunoblotted with various antibodies as indicated.

Immunoprecipitation. Top1 and Top2β were immunoprecipitated by Top1 antiserum and Top2β (H8) antibody (sc-25330), respectively, as described previously (20).

Transfection with cDNAs and siRNAs. To overexpress dominant-negative HA-tagged ubiquitins (HA-K48R, K29R, and K63R), HA-tagged wild-type ubiquitin (HA-Ub) or truncated shuttle factor (ΔUBL or ΔUBA) cells were transfected with the indicated plasmids as described previously (20). For transfections with HA-tagged plasmids, the transfection efficiency was evaluated by examining the HA levels in the transfected cells. For siRNA transfection, 250 pmol of siRNAs was transfected into HeLa cells (50% confluent in 100-mm plates) using the Oligofectamine transfection reagent (Invitrogen). Forty-eight hours after transfection, cells were reseeded in 35-mm plates. VP-16-induced Top2β and CPT-induced Top1 degradations were examined 72 h posttransfection.

Formaldehyde cross-linking of chromosomal proteins to DNA. HeLa cells were pretreated with MG132 (5 μM) or with DRB (150 μM) for 30 min, followed by treatment with increasing concentrations of VP-16 (0, 10, and 150 μM) for another 90 min. Subsequently, cells were cross-linked with 1% formaldehyde at room temperature for 10 min. Cross-linking was terminated by adding 0.125 M glycine to the media. Cells were then washed 3 times with ice-cold phosphate-buffered saline (PBS) and lysed either directly with 80 μl 6× SDS sample buffer or with 100 μl alkaline lysis buffer. Alkaline lysates were subjected to staphylococcal S7 nuclease digestion as described above. Cell lysates with or without staphylococcal S7 nuclease digestion were subjected to SDS-PAGE, followed by immunoblotting with specific antibodies against Top2β, RNAPII, or individual proteasome subunits. To obtain the insoluble chromatin-containing fraction of formaldehyde cross-linked cells, the cells were incubated with ice-cold 1× radioimmunoprecipitation assay (RIPA) buffer supplemented with a cocktail of protease inhibitors and 1 mM phenylmethylsulfonyl fluoride (PMSF) for 10 min to disrupt both the cellular membrane and nuclear envelope. The incubation was followed by collecting the cells using a rubber policeman and an immediate centrifugation at 200 × *g* at 4°C for 15 min. Pellets which contain insoluble chromosomal DNA were dissolved using alkaline lysis buffer (200 mM NaOH, 2 mM EDTA). Following neutralization, staphylococcal S7 nuclease digestion and immunoblotting were performed as described above.

Peptides. A dominant-negative peptide was custom synthesized (Pepnome Inc.). The reverse sequence of HIV-1 Tat_{57-49} (RRRQRRKKR) was fused to the C-terminal HbYX motif (GTPEGLYL) of the 19S ATPase Rpt2 (21, 22). A control peptide (RRRQRRKKRLGISYGRK) was custom synthesized using the reverse sequence of Tat_{57-49} fused with Tat_{50-42}. Prior to the treatment with these peptides, cells were incubated with chloroquine (30 μM) for 30 min to inhibit lysosome activities (23).

RESULTS

VP-16 induces proteasomal degradation of both DNA-bound Top2β and RNAPII LS. VP-16, an anticancer agent and inducer of Top2-DNA cleavage complexes, is known to cause proteasome-dependent degradation of Top2β (8, 9). This degradation was significantly suppressed by a transcription elongation inhibitor, 5,6-dicholoro-1-β-D-ribobenzimidazole (DRB) (Fig. 1A). DRB is known to inhibit pTEFb/CDK9-mediated Ser-2 phosphorylation of the CTD of RNAPII, confining RNAPII within the promoter-proximal regions (24). Furthermore, the degradation of Top2β was also shown to require the active-site tyrosine of Top2β, which is essential for the formation of Top2β-DNA cleavage complexes. As shown in Fig. 1B, VP-16 induced efficient degradation of ectopically expressed wild-type (WT) mouse Top2β (mTop2β) but not mTop2β with a tyrosine-to-phenylalanine point mutation at its active site (Fig. 1B, anti-HA immunoblot for HA-tagged mTop2β). Moreover, VP-16 efficiently induced degradation of endogenous human Top2β (hTop2β) (Fig. 1B, anti-Top2β immunoblot) in the presence of the ectopically expressed mTop2β. These results clearly indicate that VP-16-induced degradation occurs exclusively on Top2β-DNA cleavage complexes but not on free Top2β that is not DNA bound.

Not surprisingly, the VP-16-induced degradation of RNAPII LS was shown to rely largely on the formation of Top2β-DNA cleavage complexes. The total cellular content of RNAPII LS was reduced significantly upon VP-16 treatment in $Top2\beta^{+/+}$ primary mouse embryonic fibroblasts (pMEFs). In contrast, no detectable degradation of RNAPII LS (labeled RNAPII) was observed in $top2\beta^{-/-}$ pMEFs (Fig. 1C).

The exposure of DNA double-strand breaks (DSBs) was investigated as the consequence of Top2β degradation on DNA. Phosphorylation on Ser-139 of H2AX (γ-H2AX, a key DNA damage signal induced by DSBs) was shown in $Top2\beta^{+/+}$ pMEFs upon VP-16 treatment, whereas a much reduced level of γ-H2AX was observed in $top2\beta^{-/-}$ pMEFs (Fig. 1C). Taken together, VP-16-induced DNA damage signals are dependent on the formation of Top2β-DNA cleavage complexes. In contrast, the H_2O_2-induced γ-H2AX signal appeared to be unaffected in $top2\beta^{-/-}$ pMEFs (Fig. 1D).

These results inspire a model (Fig. 1E) in which Top2β-DNA cleavage complexes act as roadblocks to the elongating RNAPII; the encounter between Top2β roadblocks and RNAPII triggers a proteasomal degradation of both Top2β and RNAPII LS on DNA, exposing the otherwise Top2β-concealed DSBs.

Top2β-DNA cleavage complexes act as protein roadblocks to elongating RNAPII. Evidence supporting the proposed model comes from an analysis of the phosphorylation state of RNAPII by

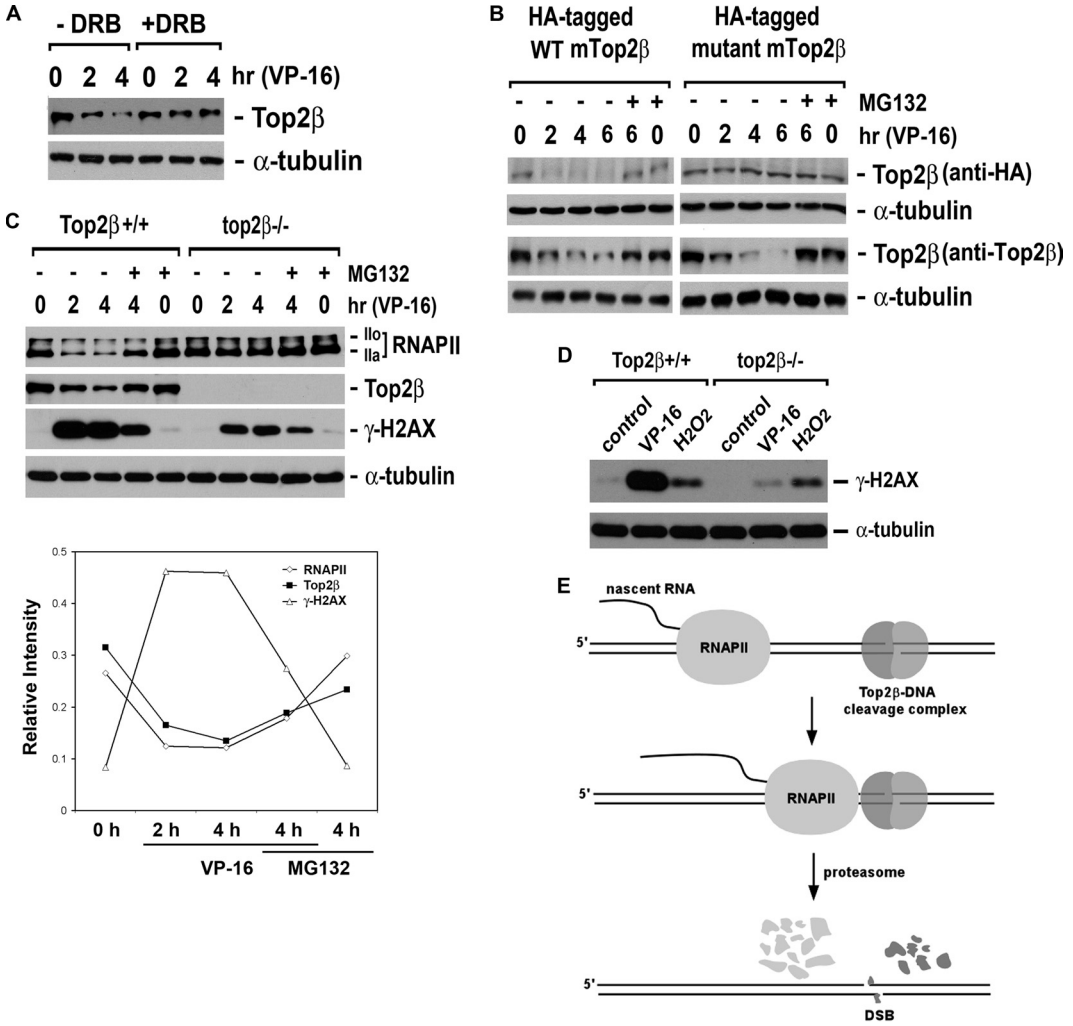

FIG 1 VP-16 induces transcription-dependent degradation of Top2β. (A) The transcription elongation inhibitor DRB abolishes VP-16-induced Top2β degradation. HeLa cells (2.5×10^5) cultured in complete DMEM were treated with 250 μM VP-16 for 0 (0.1% dimethyl sulfoxide [DMSO]), 2, or 4 h in the presence or absence of 100 μM DRB. Cell lysates were immunoblotted using specific antibody against Top2β or α-tubulin. (B) VP-16-induced Top2β degradation requires the active-site tyrosine of Top2β. HeLa cells were transfected with the plasmid (pYLL201) expressing HA-tagged WT mTop2β or the plasmid (pYLL204) expressing HA-tagged active-site mutant mTop2β (Y814F). Twenty-four hours posttransfection, cells were treated with 250 μM VP-16 in the presence or absence of 5 μM MG132 for various time periods as indicated. Cell lysates were prepared and immunoblotted with the anti-HA antibody for detecting ectopically expressed mTop2β or anti-Top2β antibody for detecting endogenous total Top2β. (C) VP-16 induces Top2β-dependent degradation of RNAPII LS and the γ-H2AX signal. Primary Top2β$^{+/+}$ and top2β$^{-/-}$ MEFs cultured in DMEM supplemented with 0.2% FetalPlex were treated with 250 μM VP-16 for 0, 2, or 4 h in the presence or absence of MG132. Cell lysates were analyzed by immunoblotting using specific antibodies against RNAPII LS, Top2β, γ-H2AX, or α-tubulin. (Bottom) Quantification of relative intensities of immunoreactive bands in wild-type pMEFs treated with VP-16 in the presence or absence of MG132 as shown above. (D) H_2O_2-induced γ-H2AX is independent of Top2β. Primary Top2β$^{+/+}$ and top2β$^{-/-}$ MEFs were treated with 0.1% DMSO, 100 μM VP-16, or 500 μM H_2O_2 for 1 h. Cell lysates were analyzed by immunoblotting using antibodies against γ-H2AX or α-tubulin. (E) A proposed model for VP-16-induced Top2β degradation. Top2β-DNA cleavage complexes arrest elongating RNAPII, triggering a proteasomal degradation of both Top2β and RNAPII LS on DNA. Degradation of Top2β results in exposure of the otherwise Top2β-concealed DNA DSBs.

analyzing the relative distribution of IIo (hyperphosphorylated) and IIa (hypophosphorylated) forms of RNAPII in VP-16-treated HeLa cells. The CTD of RNAPII typically consists of up to 52 repeats of the sequence Tyr-Ser-Pro-Thr-Ser-Pro-Ser (25), and phosphorylation occurs primarily on Ser-2 and Ser-5 (5). It is widely held that the promoter binding and other early events of transcription are carried out by RNAPIIa, while elongation is carried out by RNAPIIo (26, 27).

In the presence of the proteasome inhibitor MG132, VP-16 caused a significant shift of RNAPII from the IIa form to the IIo form (Fig. 2A), which is indicative of elongation arrest. This shift was associated with an elevated phosphorylation of Ser-2 (Fig. 2A), bolstering the elongation arrest. An inhibitor of CTD kinase pTEFb/cyclin-dependent kinase 9 (CDK9), DRB, was employed in subsequent experiments to sequester the initiated RNAPII in the promoter-proximal regions, thereby preventing its interaction with Top2β-DNA cleavage complexes within the transcribed regions. As shown in Fig. 2A, in HeLa cells pretreated with DRB, a IIa-to-IIo shift as well as Ser-2 phosphorylation of RNAPII was no longer observed upon VP-16 treatment. However, at the DRB concentration (150 μM) used in this experiment, transcription initiation is also likely inhibited.

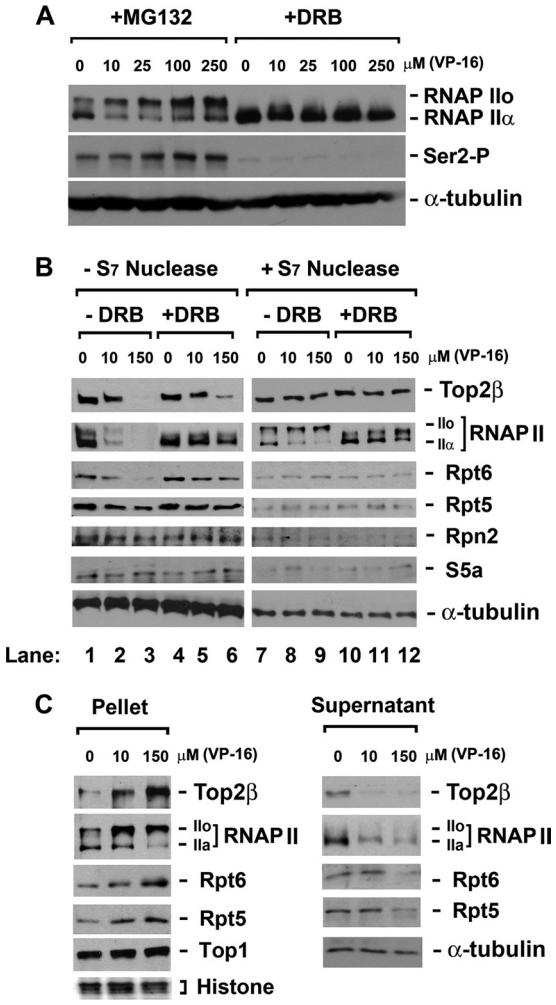

FIG 2 VP-16 induces accumulation of RNAPIIo and 19S ATPase subunits (Rpt proteins) on chromatin. (A) VP-16 induces accumulation of hyperphosphorylated RNAP II (IIo). HeLa cells were treated with VP-16 at the indicated concentrations in the presence of either 5 μM MG132 (to prevent the degradation of RNAPII LS) or 150 μM DRB (to prevent transcription elongation) for 2 h. Cell lysates were analyzed by immunoblotting using specific antibodies against RNAPII, Ser-2-phosphorylated RNAPII, or α-tubulin. (B) VP-16 treatment increases the cross-linking of Top2β, RNAPII, and RNAPII-associated 19S ATPases to chromosomal DNA in a transcription-dependent manner. DNA-bound proteins were cross-linked to chromosomal DNA using 1% formaldehyde upon drug treatment (0, 10, or 150 μM VP-16 in the presence of MG132 or DRB for 90 min). Cell lysates were either directly analyzed by immunoblotting or subjected to S7 nuclease digestion before immunoblotting with antibodies against RNAPII, Top2β, Rpt6, Rpt5, Rpn2, S5a, or α-tubulin. (C) Chromosomal DNA-containing pellets from formaldehyde-treated cells display accumulation of Top2β, RNAPII, Rpt6, and Rpt5 in response to VP-16, while the corresponding supernatants show the opposite. HeLa cells were treated and cross-linked as described for panel B. Cell lysates were then separated into chromosomal DNA pellets and supernatants by differential centrifugation. The cell pellets were subjected to S7 nuclease digestion. Both the supernatants and the S7-digested pellets were analyzed by immunoblotting with specific antibodies against RNAPII, Top2β, Rpt6, Rpt5, Top1 (a loading control for pellets), or α-tubulin (a loading control for supernatants). Histones (another loading control for pellets) were stained by Ponceau S.

To confirm that VP-16-induced accumulation of elongating RNAPII occurs on chromatin, a cross-linking experiment was performed. Briefly, VP-16-treated HeLa cells were treated with 1% formaldehyde to cross-link chromatin-bound proteins to DNA. The disappearance of DNA-bound protein from SDS-PAGE gel was expected, because the cross-linked protein-DNA (chromatin) complexes are too large to enter the gel. VP-16 induced a concentration-dependent disappearance of both Top2β and RNAPII LS from the SDS-PAGE gel (Fig. 2B, lanes 1 to 3). Top2β disappeared as expected, since VP-16 is known to stabilize Top2β-DNA cleavage complexes and recruit Top2β from its nucleolar storage sites to chromatin (28). The disappearance of RNAPII LS is interesting and suggests the accumulation of RNAPII on chromatin upon encountering Top2β-DNA cleavage complexes. When sequestered within the promoter-proximal regions by DRB, RNAPII LS accumulated on chromatin to a much lesser extent despite unaffected formation of Top2β-DNA cleavage complexes, as evidenced by the reduced amount of DNA cross-linked RNAPII LS but comparable amount of DNA cross-linked Top2β in the presence of DRB (Fig. 2B, lanes 4 to 6).

As a control, the total lysate of formaldehyde-treated cells was digested with staphylococcal S7 nuclease to release proteins from cross-linked protein-DNA complexes prior to SDS-PAGE. As shown in Fig. 2B, lanes 7 to 12, S7 nuclease treatment released both RNAPIIo and Top2β from DNA, as evidenced by their reappearance on immunoblots.

To further verify the RNAPII accumulation on chromosomal DNA, we fractionated the total cell lysates (cross-linked) into supernatants and insoluble chromatin pellets by differential centrifugation. The supernatants displayed decreased amounts of Top2β and RNAPII in response to increasing concentrations of VP-16. In contrast, DNA pellets (after staphylococcal S7 nuclease treatment) displayed increasing amounts of Top2β and RNAPII in response to the increasing concentrations of VP-16 (Fig. 2C). Collectively, our results indicate that Top2β-DNA cleavage complexes trigger the accumulation of RNAPII on chromatin and support a model in which Top2β-DNA cleavage complexes act as roadblocks to the elongating RNAPII.

Given that 19S ATPases are part of the elongating complex of RNAPII (13–16), we were not surprised to find that the 19S ATPase subunits (Rpt5 and Rpt6) also accumulated on chromosomal DNA in response to the increasing concentrations of VP-16 (Fig. 2B, lanes 1 to 3). DRB counteracted this VP-16-induced accumulation (Fig. 2B, lanes 4 to 6). The non-ATPase subunits of 19S proteasome (Rpn2 and S5a) were not cross-linked to DNA under the same conditions (Fig. 2B, lanes 1 to 3). As a control, staphylococcal S7 nuclease caused full recovery of the 19S ATPases (Fig. 2B, lanes 7 to 12). Consistently, analysis of fractionated supernatant and DNA pellets confirmed the VP-16-induced accumulation of 19S ATPases on DNA (Fig. 2C). In aggregate, Top2β-DNA cleavage complexes arrest RNAPII and RNAPII-associated 19S ATPases on chromatin.

The clearance of Top2β-DNA cleavage complexes is mediated by 20S proteasome independently of Ub. As proteasome inhibitors are known to abolish the degradation of Top2β-DNA cleavage complexes (8, 9), the siRNA-mediated silencing of POMP (proteasome maturation protein) further substantiated the participation of 20S proteasome. POMP, also known as hUmp1, acts as a chaperone that guides two α7β7 half proteasomes to assemble into the mature 20S core (29). Silencing POMP expression in HeLa cells has been shown to cause a considerable decrease in proteasomal hydrolyzing activity (30). siRNA-mediated silencing of POMP completely abolished the degradation of Top2β-DNA cleavage complexes in HeLa cells

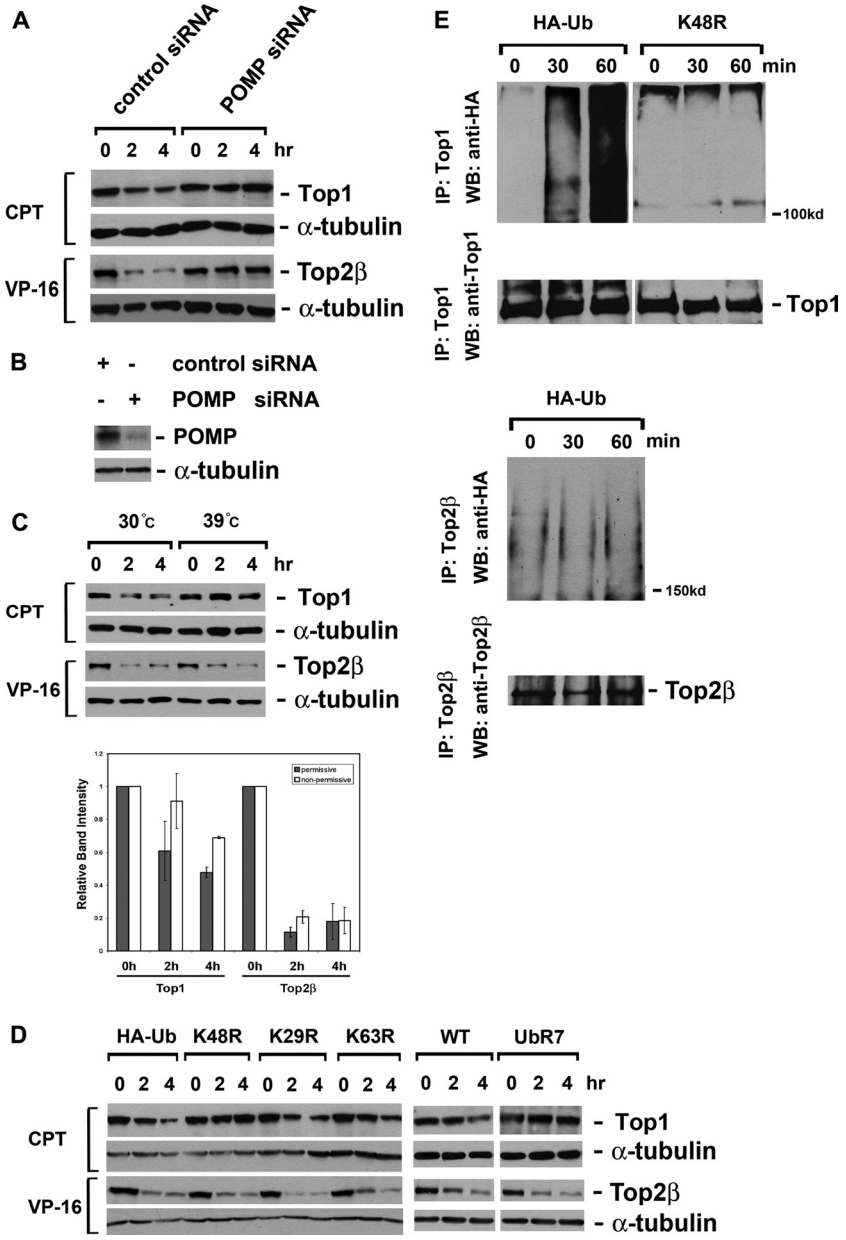

FIG 3 VP-16-induced degradation of Top2β requires the mature 20S proteasome but not Ub. (A) Disrupting the maturation of the 20S proteasome abrogates VP-16-induced degradation of Top2β. HeLa cells were transfected with control siRNA or POMP siRNA. Seventy-two hours posttransfection, cells were treated with either 250 μM VP-16 or 25 μM CPT for 0, 2, or 4 h. Cell lysates were immunoblotted with anti-Top1, anti-Top2β, or α-tubulin antibody. (B) Analysis of POMP protein level. Seventy-two hours posttransfection, cell lysates were immunoblotted with anti-POMP or α-tubulin antibody. (C) VP-16-induced degradation of Top2β does not require the major E1. Mouse ts85 cells were treated with 250 μM VP-16 or 25 μM CPT for 0, 2, or 4 h at either the permissive (30°C) or the nonpermissive (39°C) temperature. Cell lysates were then analyzed by immunoblotting as described for panel A. (Bottom) Quantification of relative intensities of immunoreactive bands as shown above. (D) Expression of dominant-negative mutant Ubs does not impact VP-16-induced degradation of Top2β. HeLa cells were transfected with plasmids expressing either HA-tagged WT Ub or HA-tagged mutant Ubs. Twenty-four hours posttransfection, cells were treated with either 250 μM VP-16 or 25 μM CPT for 0, 2, or 4 h. Cell lysates were immunoblotted as described for panel A. (E) Analysis of the formation of poly-Ub-Top2β conjugates in VP-16-treated cells. HeLa cells were transfected with a plasmid expressing HA-tagged Ub (K48R or WT). Twenty-four hours posttransfection, cells were treated with either 250 μM VP-16 or 25 μM CPT for 0, 30, or 60 min. Standard immunoprecipitation was performed using anti-Top1 or anti-Top2β antibody. Immunoblotting was performed using anti-HA, anti-Top1, or anti-Top2β antibody.

(Fig. 3A). Camptothecin (CPT)-induced proteasomal degradation of topoisomerase I (Top1) served as a positive control (Fig. 3A) (18). The efficiency of POMP siRNA silencing was examined by immunoblotting against POMP (Fig. 3B).

Paradoxically, the degradation of Top2β-DNA cleavage complexes appeared to be Ub independent. First, in ts85 cells that harbor a temperature-sensitive major E1 (19), the degradation of Top2β at the nonpermissive temperature was as efficient as that observed at the permissive temperature. In contrast, CPT-induced, Ub-dependent degradation of Top1 (18, 20) was com-

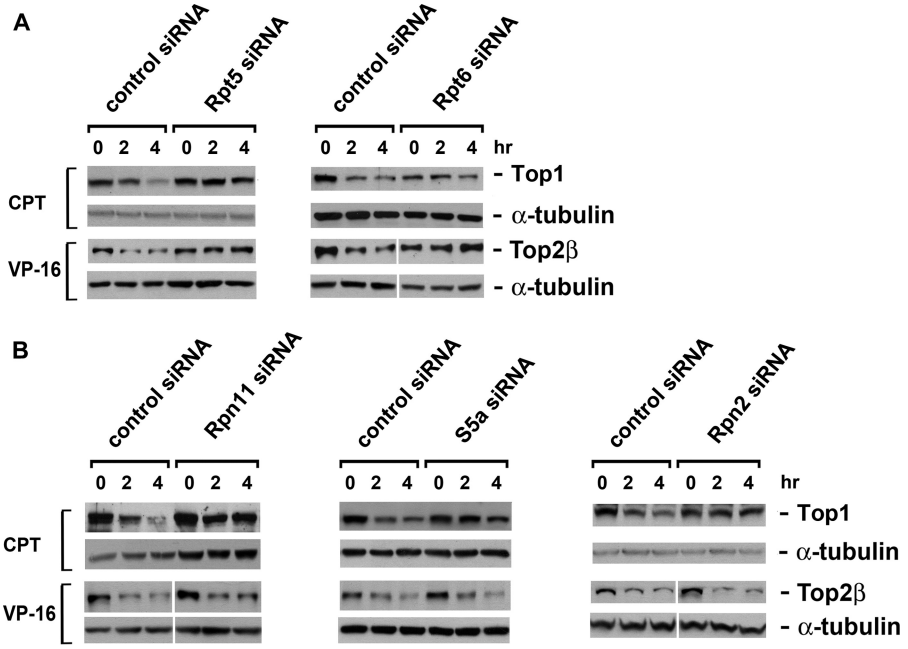

FIG 4 VP-16-induced degradation of Top2β requires 19S ATPases but not the entire 19S regulatory particle. (A) siRNA-mediated silencing of 19S ATPase subunits (Rpt5 and Rpt6) abolishes VP-16-induced degradation of Top2β. HeLa cells were transfected with control, Rpt5, or Rpt6 siRNA. Seventy-two hours posttransfection, cells were treated with 250 μM VP16 or 25 μM CPT for 0, 2, or 4 h. Cell lysates were immunoblotted with antibody against Top1, Top2β, or α-tubulin. (B) siRNA-mediated silencing of the non-ATPase components of the19S regulatory particle does not impact VP-16-induced degradation of Top2β. HeLa cells were transfected with control, Rpn11, S5a, or Rpn2 siRNA, followed by drug treatment and immunoblotting as described for panel A.

pletely abolished at the nonpermissive temperature (Fig. 3C). Second, a series of plasmid-encoded, branch point-mutated Ubs were introduced into HeLa cells by transient transfection; when overexpressed in cells, none of these dominant-negative mutant Ubs affected VP-16-induced degradation of Top2β. However, the Lys-48-mutated Ubs (K48R and UbR7) completely abolished Ub-dependent Top1 degradation induced by CPT (Fig. 3D) (20). These results indicate that the degradation of Top2β requires neither single Ub conjugation via major E1 nor the formation of Lys-48-, Lys-29-, or Lys-63-linked poly-Ub chains. We also examined the existence of poly-Ub-Top2β conjugates, or the lack of them, in VP-16-treated HeLa cells. VP-16 did not induce Top2β-poly-Ub conjugates, while CPT induced extensive poly-Ub-Top1 conjugates under the same condition. Those poly-Ub-Top1 conjugates disappeared when K48R Ubs were overexpressed in the cells (Fig. 3E), confirming that the conjugate of Top1 contains the Lys-48-linked poly-Ub chain. In aggregate, our results strongly suggest that the proteasomal degradation of Top2β roadblocks is Ub independent.

The degradation of Top2β-DNA cleavage complexes requires 19S ATPases but not the entire 19S regulatory particle. Proteins could take a Ub-free route to the proteasome for degradation. These proteins fall into three categories: (i) small proteins with an unstructured terminus or a terminus with a binding site for the α7 subunit of the 20S proteasome (31–33), (ii) a native protein or a protein complex bearing a hydrophobic patch that mimics a poly-Ub chain (34) (it has been shown that both the poly-Ub chain and the poly-Ub-mimicking sequences could be shielded from poly-Ub receptors by excessive UBA domains of the shuttle factor Rad23 [ΔUBL] [35, 36]), and (iii) a protein substrate of PA28γ-20S proteasome, which does not require the poly-Ub chain, as a degradation permit (37).

Due to the large size of the Top2β homodimer (~360 kDa), it does not fall into the first category. Interestingly, Top2β does not fit the remaining two categories either, as neither the overexpression of truncated shuttle factors (ΔUBL Rad23) nor the silencing of PA28γ by siRNA could influence the proteasomal degradation of Top2β (see Fig. S1A and B in the supplemental material). Thus, a question emerges as to whether or not the classical 26S proteasome is the degradation machinery for Top2β. To answer this question, we knocked down a series of 19S components using their respective siRNAs. Only siRNAs that target 19S ATPases (S6a/Rpt5 and Sug1/Rpt6) significantly hindered the degradation of Top2β (Fig. 4A). The siRNA targeting the 19S lid component S13/Rpn11, the 19S base-lid connector Rpn10/S5a, or the non-ATPase base component p110/Rpn2 was unable to influence the degradation of Top2β (Fig. 4B). In contrast, CPT-induced Top1 degradation was shown to require all of the tested 19S components (Fig. 4A and B). The knockdown efficiency of each siRNA was confirmed by the decrease of its corresponding protein and the accumulation of Ub conjugates (see Fig. S2A and B in the supplemental material). Taken together, our results suggest that only the 20S core and 19S ATPases, but not the entire 26S proteasome, are required for the clearance of Top2β roadblocks.

The degradation of Top2β-DNA cleavage complexes requires 20S core-mediated assembly of the 19S ATPase ring. Several studies have demonstrated that 19S ATPases dock onto 20S proteasome by inserting their C termini into the corresponding inter-α-subunit pockets of the 20S proteasome α ring (21, 38). The assembly of the 19S ATPase ring is guided by three chaperones (Rpn14/PAAF1, Nas6/P28, and Hsm3/S5b) and a template (20S α ring) (39–43).

Since both 19S ATPases and 20S proteasome are required for the transcription-dependent degradation of Top2β, an important

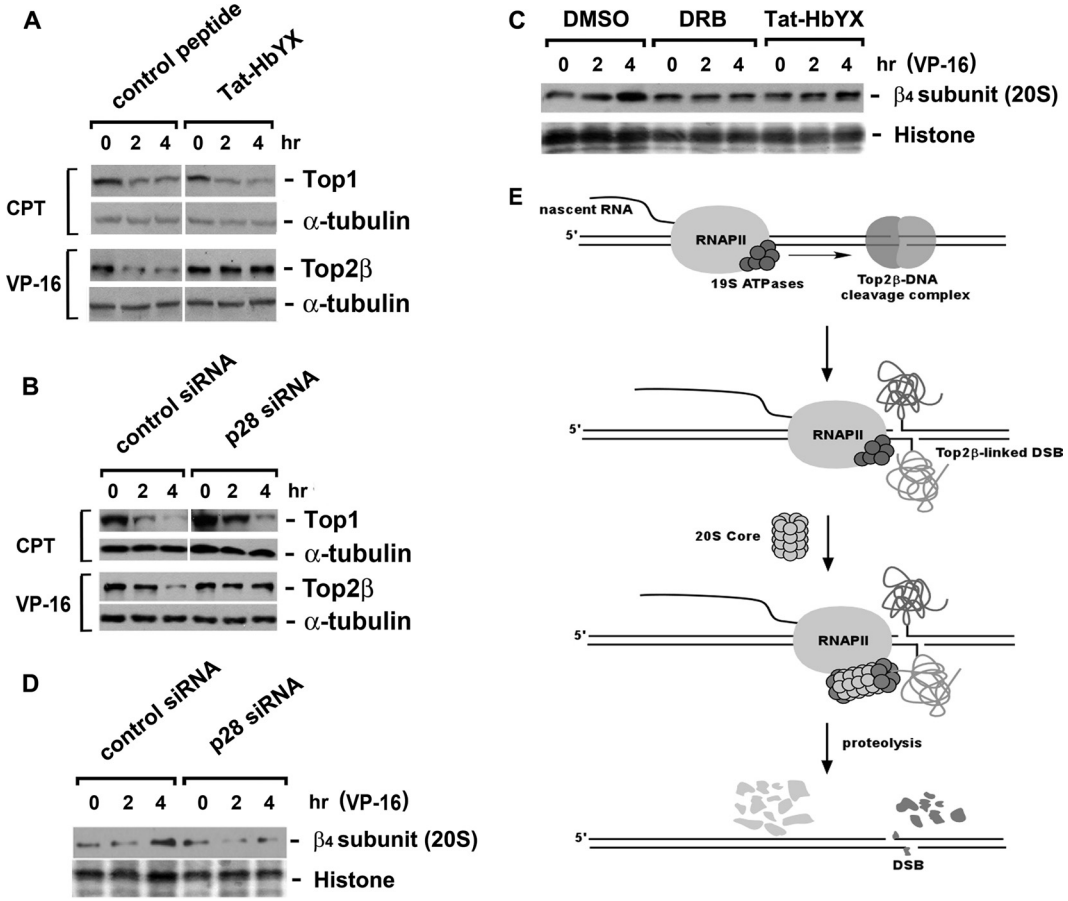

FIG 5 VP-16-induced degradation of Top2β requires 20S-mediated assembly of 19S ATPase ring. (A) Rpt2 C terminus-derived peptide (Tat-HbYX) abolishes VP-16-induced degradation of Top2β. HeLa cells were treated with the dominant-negative peptide Tat-HbYX (100 μM) for 45 min, followed by cotreatment with 250 μM VP-16 or 25 μM CPT for 0, 2, or 4 h. Cell lysates were immunoblotted with antibody against Top1, Top2β, or α-tubulin. (B) siRNA-mediated silencing of the assembly chaperone p28 reduces VP-16-induced degradation of Top2β. HeLa cells were transfected with p28/Nas6 siRNA. Seventy-two hours posttransfection, drug treatment and immunoblotting were performed as described for panel A. (C) Both DRB and Tat-HbYX peptide prevent the recruitment of 20S proteasome to chromosomal DNA. HeLa cells were pretreated with 0.1% dimethyl sulfoxide (DMSO), DRB (150 μM), or Tat-HbYX peptide (100 μM) for 45 min, followed by cotreatment with 250 μM VP-16 for 0, 2, or 4 h. The formaldehyde cross-linking was performed, and chromosomal DNA-containing pellets were collected and processed as described in the legend to Fig. 2C, followed by immunoblotting with the anti-β_4 subunit (20S proteasome) antibody. Histones were stained by Ponceau S. (D) siRNA-mediated silencing of p28 decreases chromatin-bound 20S proteasome. HeLa cells were transfected with control or p28 siRNA. Seventy-two hours posttransfection, cells were treated with 250 μM VP-16 for 0, 2, or 4 h, followed by formaldehyde cross-linking. Chromosomal DNA-containing pellets were collected, processed, and immunoblotted as described for panel C. (E) A proposed model for the interplay among elongating RNAPII, Top2β-DNA cleavage complex, and proteasome. When the elongating RNAPII stalls at the Top2β roadblock, the blocked RNAPII serves as a damage signal. The RNAPII-associated 19S ATPase recruits the 20S proteasome, resulting in the assembly of the ATPase-20S proteasome subcomplex that proteolyzes the Top2β roadblock.

question is whether they function as an assembled complex. To test this possibility, we blocked the assembly of the 19S ATPase ring using a fusion peptide consisting of the reverse sequence of HIV-1 Tat_{57-49} (RRRQRRKKR) and the C-terminal HbYX motif (GTPEGLYL) of the 19S ATPase Rpt2 (21, 22). This fusion peptide, Tat-HbYX (RRRQRRKKRGTPEGLYL), is expected to be cell membrane permeable (due to the reverse sequence of Tat_{57-49}) and capable of binding to inter-α-subunit pockets on the 20S proteasome (due to the HbYX motif), thereby acting as an efficient dominant negative to prevent the assembly of the ATPase-20S subcomplex.

In contrast to the control peptide (RRRQRRKKRLGISYGRK with no HbYX motif), Tat-HbYX completely abolished the degradation of Top2β (Fig. 5A). In line with this result, siRNA-mediated silencing of the major chaperone (Nas6/p28) for the 19S ATPase ring assembly significantly hampered Top2β degradation (Fig. 5B). These results suggest that 19S ATPase ring assembly is a necessary prerequisite for Top2β degradation. However, CPT-induced Top1 degradation, which requires mature 26S proteasome, appeared independent of a *de novo* assembly of 19S ATPase ring (Fig. 5A and B).

As the executor of destruction of protein roadblocks, 20S proteasome is anticipated to be present on DNA. Thus, the DNA cross-linking experiments described earlier were performed. The fractionated DNA pellets displayed an increase of 20S proteasome on DNA in response to VP-16 (Fig. 5C). Such an increase was shown to be transcription dependent and to require the assembly of the 19S ATPase ring, as this increase was abolished by DRB, Tat-HbYX peptide (Fig. 5C), or Nas6/p28 siRNA (Fig. 5D). Nevertheless, a noticeable temporal delay

compared to 19S ATPase subunits was observed for 20S proteasome on chromatin.

DISCUSSION

Our current studies have clarified the interplay among transcription elongation, proteasomal degradation, and exposure of DSBs when Top2β-DNA cleavage complexes manifested as protein roadblocks. Our results suggest that Top2β-DNA cleavage complexes arrest elongating RNAPII complexes, triggering a proteasomal degradation of the Top2β roadblocks and the subsequent exposure of DSBs. Most likely the exposure of DSBs is for the purpose of repair, so that the lethal cessation of transcription could be avoided. However, the unrepaired DSBs could trigger chromosomal deletions and translocations. Indeed, VP-16 has been shown to induce MLL1 translocations, leading to therapy-related acute myeloid leukemia (t-AML) (44). It has been suggested that VP-16-induced MLL1 translocation is due to proteasomal degradation of Top2β cleavage complexes and its subsequent exposure of DSBs (10). Our current results may shed light on the molecular mechanism underlying VP-16-induced secondary malignancies, ultimately leading to more efficacious use of VP-16.

Proteasome has been linked to transcription at different levels. It was originally reported that the 19S ATPases are recruited to the promoter regions (13–16). However, the 20S proteasome is only recruited when RNA polymerase is paused at the transcription termination sites (15). UV irradiation and other DNA-damaging events lead to the recruitment of the 20S proteasome within the transcribed region due to pausing of the RNA polymerase at the DNA damage sites (15, 45).

Our observations corroborate the notion that proteasome plays a proteolytic role in clearing stalled transcription machineries (15). Moreover, we have uncovered a novel Ub-independent proteasome pathway that is schematically shown in Fig. 5E. When elongating RNAPII stalls at Top2β-DNA cleavage complexes, the blocked RNAPII serves as a damage signal. The RNAPII-associated 19S ATPases are activated as an early event during the encounter for detecting the Top2β roadblocks (e.g., through DNA helicase Rpt5) (46, 47). Consequently, 20S proteasome is recruited by the 19S ATPases, resulting in Top2β degradation and revealing the otherwise Top2β-concealed DSBs for repair. The orchestration of 19S ATPases and 20S proteasome suggests a two-step mechanism for removal of the protein roadblock. Because of the limited access to the proteasome catalytic chamber inside the 20S core particle, the initial step could involve the unfolding of the protein roadblock by the RNAPII-associated 19S ATPases. The persistent arrest of RNAPII by DNA damages revealed after protein unfolding could result in the subsequent recruitment of 20S proteasome. This two-step mechanism could be decoupled when RNAPII encounters noncovalent protein-DNA complexes without DNA damage (e.g., nucleosomes). In this case, the unfolding of the noncovalent protein roadblock by 19S ATPases would allow rapid readthrough of the RNAPII, thereby obviating the recruitment of 20S proteasome and degradation of the unfolded protein. The possible role of 19S ATPases in unfolding noncovalent protein-DNA complexes could explain their involvement in transcription elongation on a DNA template covered with tightly bound proteins, such as nucleosomes (13–15).

In contrast to Top2β-DNA cleavage complexes, Top1-DNA cleavage complexes undergo degradation through a Ub-dependent pathway (20, 48). Since both complexes are covalent protein-DNA complexes, it is unclear why distinct pathways are adopted by the paused RNAPII. One possibility is that Top1-DNA complexes exist in two different polarities to the elongating RNAPII and contain a protein-concealed single-strand break (SSB) that can be located on either the template or the nontemplate strand. RNAPII may elicit two different responses depending on the polarity of the Top1 roadblock. As shown in Fig. S3 in the supplemental material, 19S ATPases have been demonstrated to be part of the elongating RNAPII complex (13–16). Armed with these ATP-hydrolyzing enzymes, RNAPII may read through the Top1 roadblock on the nontemplate strand (coding strand) by unfolding/removing Top1 from the template strand. Excision of such an unfolded Top1 behind the elongating RNAPII may occur through Tdp1 (49, 50). In contrast, RNAPII is likely to remain paused at the Top1 roadblock on the template strand. In this case, Top1 could be degraded by the same Ub-independent pathway as that utilized to degrade Top2β roadblocks. The observation of Ub dependency may simply reflect the relative rates of the two degradation processes responsible for clearing/removing Top1 roadblocks.

ACKNOWLEDGMENTS

This work was supported by NIH grants RO1 CA039662 and RO1 CA102463.

We thank Kiran Madura (Rutgers University) and James Wang (Harvard University) for insightful discussion and suggestions. We are also grateful to Cam Patterson, Michelle Pagano, and Christine Blattner for providing various plasmids.

REFERENCES

1. **Ratner JN, Balasubramanian B, Corden J, Warren SL, Bregman DB.** 1998. Ultraviolet radiation-induced ubiquitination and proteasomal degradation of the large subunit of RNA polymerase II. Implications for transcription-coupled DNA repair. J. Biol. Chem. **273:**5184–5189.
2. **Svejstrup JQ.** 2007. Contending with transcriptional arrest during RNAPII transcript elongation. Trends Biochem. Sci. **32:**165–171.
3. **Anindya R, Aygun O, Svejstrup JQ.** 2007. Damage-induced ubiquitylation of human RNA polymerase II by the ubiquitin ligase Nedd4, but not Cockayne syndrome proteins or BRCA1. Mol. Cell **28:**386–397.
4. **Luo Z, Zheng J, Lu Y, Bregman DB.** 2001. Ultraviolet radiation alters the phosphorylation of RNA polymerase II large subunit and accelerates its proteasome-dependent degradation. Mutat. Res. **486:**259–274.
5. **Dahmus ME.** 1995. Phosphorylation of the C-terminal domain of RNA polymerase II. Biochim. Biophys. Acta **1261:**171–182.
6. **Harreman M, Taschner M, Sigurdsson S, Anindya R, Reid J, Somesh B, Kong SE, Banks CA, Conaway RC, Conaway JW, Svejstrup JQ.** 2009. Distinct ubiquitin ligases act sequentially for RNA polymerase II polyubiquitylation. Proc. Natl. Acad. Sci. U. S. A. **106:**20705–20710.
7. **Somesh BP, Reid J, Liu WF, Sogaard TM, Erdjument-Bromage H, Tempst P, Svejstrup JQ.** 2005. Multiple mechanisms confining RNA polymerase II ubiquitylation to polymerases undergoing transcriptional arrest. Cell **121:**913–923.
8. **Mao Y, Desai SD, Ting CY, Hwang J, Liu LF.** 2001. 26S proteasome-mediated degradation of topoisomerase II cleavable complexes. J. Biol. Chem. **276:**40652–40658.
9. **Zhang A, Lyu YL, Lin CP, Zhou N, Azarova AM, Wood LM, Liu LF.** 2006. A protease pathway for the repair of topoisomerase II-DNA covalent complexes. J. Biol. Chem. **281:**35997–36003.
10. **Azarova AM, Lyu YL, Lin CP, Tsai YC, Lau JY, Wang JC, Liu LF.** 2007. Roles of DNA topoisomerase II isozymes in chemotherapy and secondary malignancies. Proc. Natl. Acad. Sci. U. S. A. **104:**11014–11019.
11. **Lyu YL, Kerrigan JE, Lin CP, Azarova AM, Tsai YC, Ban Y, Liu LF.** 2007. Topoisomerase IIbeta mediated DNA double-strand breaks: implications in doxorubicin cardiotoxicity and prevention by dexrazoxane. Cancer Res. **67:**8839–8846.
12. **Zhang S, Liu X, Bawa-Khalfe T, Lu LS, Lyu YL, Liu LF, Yeh ET.** 2012.

Identification of the molecular basis of doxorubicin-induced cardiotoxicity. Nat. Med. **18:**1639–1642.
13. **Gonzalez F, Delahodde A, Kodadek T, Johnston SA.** 2002. Recruitment of a 19S proteasome subcomplex to an activated promoter. Science **296:**548–550.
14. **Ferdous A, Kodadek T, Johnston SA.** 2002. A nonproteolytic function of the 19S regulatory subunit of the 26S proteasome is required for efficient activated transcription by human RNA polymerase II. Biochemistry **41:**12798–12805.
15. **Gillette TG, Gonzalez F, Delahodde A, Johnston SA, Kodadek T.** 2004. Physical and functional association of RNA polymerase II and the proteasome. Proc. Natl. Acad. Sci. U. S. A. **101:**5904–5909.
16. **Muratani M, Tansey WP.** 2003. How the ubiquitin-proteasome system controls transcription. Nat. Rev. Mol. Cell Biol. **4:**192–201.
17. **Shero JH, Bordwell B, Rothfield NF, Earnshaw WC.** 1986. High titers of autoantibodies to topoisomerase I (Scl-70) in sera from scleroderma patients. Science **231:**737–740.
18. **Desai SD, Li TK, Rodriguez-Bauman A, Rubin EH, Liu LF.** 2001. Ubiquitin/26S proteasome-mediated degradation of topoisomerase I as a resistance mechanism to camptothecin in tumor cells. Cancer Res. **61:**5926–5932.
19. **Mayer A, Gropper R, Schwartz AL, Ciechanover A.** 1989. Purification, characterization, and rapid inactivation of thermolabile ubiquitin-activating enzyme from the mammalian cell cycle mutant ts85. J. Biol. Chem. **264:**2060–2068.
20. **Lin CP, Ban Y, Lyu YL, Desai SD, Liu LF.** 2008. A ubiquitin-proteasome pathway for the repair of topoisomerase I-DNA covalent complexes. J. Biol. Chem. **283:**21074–21083.
21. **Smith DM, Chang SC, Park S, Finley D, Cheng Y, Goldberg AL.** 2007. Docking of the proteasomal ATPases' carboxyl termini in the 20S proteasome's alpha ring opens the gate for substrate entry. Mol. Cell **27:**731–744.
22. **Howl J, Jones S.** 2009. Transport molecules using reverse sequence HIV-Tat polypeptides: not just any old Tat? (WO200808225). Expert Opin. Ther. Pat. **19:**1329–1333.
23. **Abes S, Moulton H, Turner J, Clair P, Richard JP, Iversen P, Gait MJ, Lebleu B.** 2007. Peptide-based delivery of nucleic acids: design, mechanism of uptake and applications to splice-correcting oligonucleotides. Biochem. Soc. Trans. **35:**53–55.
24. **Yamaguchi Y, Wada T, Handa H.** 1998. Interplay between positive and negative elongation factors: drawing a new view of DRB. Genes Cells **3:**9–15.
25. **Meinhart A, Cramer P.** 2004. Recognition of RNA polymerase II carboxy-terminal domain by 3′-RNA-processing factors. Nature **430:**223–226.
26. **Cadena DL, Dahmus ME.** 1987. Messenger RNA synthesis in mammalian cells is catalyzed by the phosphorylated form of RNA polymerase II. J. Biol. Chem. **262:**12468–12474.
27. **Payne JM, Laybourn PJ, Dahmus ME.** 1989. The transition of RNA polymerase II from initiation to elongation is associated with phosphorylation of the carboxyl-terminal domain of subunit IIa. J. Biol. Chem. **264:**19621–19629.
28. **Christensen MO, Larsen MK, Barthelmes HU, Hock R, Andersen CL, Kjeldsen E, Knudsen BR, Westergaard O, Boege F, Mielke C.** 2002. Dynamics of human DNA topoisomerases IIalpha and IIbeta in living cells. J. Cell Biol. **157:**31–44.
29. **Fricke B, Heink S, Steffen J, Kloetzel PM, Kruger E.** 2007. The proteasome maturation protein POMP facilitates major steps of 20S proteasome formation at the endoplasmic reticulum. EMBO Rep. **8:**1170–1175.
30. **Heink S, Ludwig D, Kloetzel PM, Kruger E.** 2005. IFN-gamma-induced immune adaptation of the proteasome system is an accelerated and transient response. Proc. Natl. Acad. Sci. U. S. A. **102:**9241–9246.
31. **Chen X, Chi Y, Bloecher A, Aebersold R, Clurman BE, Roberts JM.** 2004. N-acetylation and ubiquitin-independent proteasomal degradation of p21(Cip1). Mol. Cell **16:**839–847.
32. **Sdek P, Ying H, Chang DL, Qiu W, Zheng H, Touitou R, Allday MJ, Xiao ZX.** 2005. MDM2 promotes proteasome-dependent ubiquitin-independent degradation of retinoblastoma protein. Mol. Cell **20:**699–708.
33. **Touitou R, Richardson J, Bose S, Nakanishi M, Rivett J, Allday MJ.** 2001. A degradation signal located in the C-terminus of p21WAF1/CIP1 is a binding site for the C8 alpha-subunit of the 20S proteasome. EMBO J. **20:**2367–2375.
34. **Zhang M, Pickart CM, Coffino P.** 2003. Determinants of proteasome recognition of ornithine decarboxylase, a ubiquitin-independent substrate. EMBO J. **22:**1488–1496.
35. **Glockzin S, Ogi FX, Hengstermann A, Scheffner M, Blattner C.** 2003. Involvement of the DNA repair protein hHR23 in p53 degradation. Mol. Cell. Biol. **23:**8960–8969.
36. **Raasi S, Pickart CM.** 2003. Rad23 ubiquitin-associated domains (UBA) inhibit 26S proteasome-catalyzed proteolysis by sequestering lysine 48-linked polyubiquitin chains. J. Biol. Chem. **278:**8951–8959.
37. **Li X, Lonard DM, Jung SY, Malovannaya A, Feng Q, Qin J, Tsai SY, Tsai MJ, O'Malley BW.** 2006. The SRC-3/AIB1 coactivator is degraded in a ubiquitin- and ATP-independent manner by the REGgamma proteasome. Cell **124:**381–392.
38. **Rabl J, Smith DM, Yu Y, Chang SC, Goldberg AL, Cheng Y.** 2008. Mechanism of gate opening in the 20S proteasome by the proteasomal ATPases. Mol. Cell **30:**360–368.
39. **Besche HC, Peth A, Goldberg AL.** 2009. Getting to first base in proteasome assembly. Cell **138:**25–28.
40. **Le Tallec B, Barrault MB, Guerois R, Carre T, Peyroche A.** 2009. Hsm3/S5b participates in the assembly pathway of the 19S regulatory particle of the proteasome. Mol. Cell **33:**389–399.
41. **Park S, Roelofs J, Kim W, Robert J, Schmidt M, Gygi SP, Finley D.** 2009. Hexameric assembly of the proteasomal ATPases is templated through their C termini. Nature **459:**866–870.
42. **Roelofs J, Park S, Haas W, Tian G, McAllister FE, Huo Y, Lee BH, Zhang F, Shi Y, Gygi SP, Finley D.** 2009. Chaperone-mediated pathway of proteasome regulatory particle assembly. Nature **459:**861–865.
43. **Kaneko T, Hamazaki J, Iemura S, Sasaki K, Furuyama K, Natsume T, Tanaka K, Murata S.** 2009. Assembly pathway of the mammalian proteasome base subcomplex is mediated by multiple specific chaperones. Cell **137:**914–925.
44. **Felix CA.** 1998. Secondary leukemias induced by topoisomerase-targeted drugs. Biochim. Biophys. Acta **1400:**233–255.
45. **Jacquemont C, Taniguchi T.** 2007. Proteasome function is required for DNA damage response and fanconi anemia pathway activation. Cancer Res. **67:**7395–7405.
46. **Ishizuka T, Satoh T, Monden T, Shibusawa N, Hashida T, Yamada M, Mori M.** 2001. Human immunodeficiency virus type 1 Tat binding protein-1 is a transcriptional coactivator specific for TR. Mol. Endocrinol. **15:**1329–1343.
47. **Satoh T, Ishizuka T, Tomaru T, Yoshino S, Nakajima Y, Hashimoto K, Shibusawa N, Monden T, Yamada M, Mori M.** 2009. Tat-binding protein-1 (TBP-1), an ATPase of 19S regulatory particles of the 26S proteasome, enhances androgen receptor function in cooperation with TBP-1-interacting protein/Hop2. Endocrinology **150:**3283–3290.
48. **Desai SD, Zhang H, Rodriguez-Bauman A, Yang JM, Wu X, Gounder MK, Rubin EH, Liu LF.** 2003. Transcription-dependent degradation of topoisomerase I-DNA covalent complexes. Mol. Cell. Biol. **23:**2341–2350.
49. **Pouliot JJ, Yao KC, Robertson CA, Nash HA.** 1999. Yeast gene for a Tyr-DNA phosphodiesterase that repairs topoisomerase I complexes. Science **286:**552–555.
50. **Yang SW, Burgin AB, Jr, Huizenga BN, Robertson CA, Yao KC, Nash HA.** 1996. A eukaryotic enzyme that can disjoin dead-end covalent complexes between DNA and type I topoisomerases. Proc. Natl. Acad. Sci. U. S. A. **93:**11534–11539.